Journal of
Ceramic Science
and Technology

*J. Ceram. Sci. Tech.*, **05** [01] 57-62 (2014)
DOI: 10.4416/JCST2013-00046
available online at: http://www.ceramic-science.com


# Synthesis and Characterization of Sol-Gel-Derived Chemical Mullite

**J. Roy*[1], S. Maitra[2]**

[1]Camellia Institute of Technology, Badu Road, Kolkata-700129, India
[2]Government College of Engineering & Ceramic Technology, Kolkata-700010, India
received December 29, 2013; received in revised form February 9, 2014; accepted February 13, 2014

**Abstract**

**Mullite ($3Al_2O_3{\cdot}2SiO_2$) precursor gel was synthesized using aluminum nitrate nonahydrate and liquid sodium silicate as starting materials based on the sol-gel route. The gel was characterized by means of chemical analysis, surface area and bulk density measurements. Fourier transformation infrared spectroscopic (FTIR) and differential thermal analysis (DTA) were performed to study the course of mullitization. The gel was calcined at 800 °C and compacted at 100 MPa pressure. The compacted masses were sintered at different elevated temperatures and subjected to SEM and XRD analysis for microstructure and phase development studies. FTIR studies confirmed the diphasic nature of the gel during its formation. Primary mullitization started at around 980 °C with an average activation energy of ~ 772 kJ/mol. Crystallization of mullite with a lower amount of $SiO_2$ was completed after sintering at 1600 °C.**

*Keywords: Sol-gel, mullite, FTIR, differential thermal analysis, microstructure*

## I. Introduction

Mullite is a non-stoichiometric aluminosilicate compound and crystallizes with the following structural formula $Al_2[Al_{2+2x}Si_{2-2x}]O_{10-x}$, where $x$ denotes the number of missing oxygen atoms in the mullite formula [1]. It is the only stable compound in the $SiO_2$-$Al_2O_3$ binary system under ambient conditions and its composition limits range from 3:2 to 2:1 [2–4]. Mullite exhibits good thermal and chemical stability, a low creep rate, reasonable toughness and strength, infrared transparency [5–7],etc. Based on these properties, mullite is used in making refractory materials, electronic packaging, thin films, window material for the mid-infrared wavelength range [8–12], etc.

The sol-gel process is one of the most advanced processes for the synthesis of mullite with high purity and better homogeneity. Mullite synthesized in processes like the sol-gel route is also termed chemical mullite [13]. Depending on the particle size, the gel can be categorized into two types: monophasic having a particle size at the atomic level and diphasic with a homogeneity scale in the nanometre range [14]. A wide range of research has been conducted on the synthesis and characterization of mullite using a sol gel process. A few of them are discussed here. Padmaja *et al.* [15,16] synthesized diphasic gel from boehmite sol and TEOS and studied the mullitization process with FTIR, XRD and DTA analysis. Al-Si spinel was formed at around 1000 °C and the spinel was converted into orthorhombic mullite crystal in the temperature range from 1200 – 1300 °C. Yu *et al.* [17] synthesized diphasic mullite precursor gel with different Al/Si ratios using aluminium chloride and tetraethyl orthosilicate (TEOS). In all samples mullite formation started at around1300 °C. Campos *et al.* [18] studied the mullitization of a diphasic gel synthesized from sodium metasilicate and aluminium nitrate by means of DTA, dynamic XRD and SEM. Plate-like mullite crystal formation was completed at around 1350 °C with an activation energy equal to 730 ± 150 kJ $mol^{-1}$. Buljan *et al.* [19] synthesized diphasic aluminosilicate gel and conducted FTIR, DSC, XRD and SEM analysis to study the mullitization process. Almost 50 % mullitization was completed in gel sintered at 990 °C for 3 h.

In most of the processes discussed above, mullite was synthesized using an organic precursor. But not much work has been reported on mullite synthesis from a diphasic gel system derived from inorganic salts [20]. So in this present investigation, inorganic salts (aluminium nitrate nonahydrate and silicic acid) were used to synthesize diphasic aluminosilicate mullite precursor gel.

## II. Experimental

### *(1) Synthesis of mullite precursor gel*

5 % (w/v) aluminum nitrate nonahydrate [$Al(NO_3)_3{\cdot}9H_2O$, (Merck, India), alumina content 12.98 % w/w] and liquid sodium silicate [sp. Gr. 1.6 and molar ratio of $Na_2O$: $SiO_2$ =1:3, (Loba Chemie, India), silica content 29.75 % w/w] were used. Silicic acid was prepared by passing a dilute solution of sodium silicate (7 % w/v) through a column packed with cation-exchanging resin (Dowex-50) at a flow rate of 200 ml/minute. The silicic acid solution was then dispersed in an ultrasonic bath to form silica sol, which was mixed with $Al(NO_3)_3{\cdot}9H_2O$ solution with maintenance of a stoichiometric alumina and silica ratio of mullite (3:2). To this mixed solution, ammonia solution (1:1) was added slowly under constant stirring until the pH of the solution reached around 9. The mixed sol was then

* Corresponding author: royj007@rediffmail.com

filtered and washed thoroughly. The sol was then aged to obtain the gel. The gel was dried at 80 °C overnight.

### *(2) Characterization*

In a first step, chemical analysis (following the specifications in ISO 21587 – 2:2007), surface area (using Twin Surface Area Analyser, Quantachrome) and bulk density measurements (using Ultrapyc 1200e helium pycnometer) of the dried gel were performed. To perform FTIR analysis, the dried gel was heat-treated at eight different temperatures from 200 to 1600 °C with 200 °C interval in each case and FTIR spectra of the dried gel and heat-treated samples were taken using Perkin-Elmer apparatus (Model: Vertex-70). Differential thermal analysis (DTA) of the dried gel was performed at four different heating rates 4, 6, 8 and 10 °C per minute from room temperature to 1400 °C with a differential thermal analyzer (Libratherm 1400, India).

The dried gel was calcined at 800 °C for 2 h and the calcined gel was compacted under 100 MPa pressure. The compacted masses were fired in an electrically heated muffle furnace at three different final temperatures, 1400, 1500 and 1600 °C (heating rate 10 °C/m up to 1000 °C and then 2 °C/m to reach final temperature), with a 2 h soaking period in each case. Scanning electron microscopic analysis of the samples was performed with an FEI Quanta microscope (US). An XRD pattern of the samples was taken with a Rigaku X-ray diffractometer with Cu target (Miniflex, Japan).

## III. Results and Discussion

The precursor gel was found to have a large surface area (70 $m^2/g$) and very low bulk density (0.27 $g/cm^3$), indicating a high surface activity. The water content of the gel was almost 30 %. So the gel was calcined in order to prevent excessive shrinkage during sintering. The alumina content in the synthesized gel was found to be slightly higher than that of the theoretical amount (3:2). The advantage was that this would prevent formation of glassy phase during sintering.

In the FTIR spectra of the dried gel shown in Figs. 1a and 1b, the characteristic peaks corresponding to Si-O-Si and Al-O-Al stretching vibration appeared at 477 and 747 $cm^{-1}$ respectively. The band that appeared at 3151 $cm^{-1}$ was assigned to Al-OH stretching vibration. The peak corresponding to Al-OH bending and Si-O-Si stretching vibrations overlapped at 1104 $cm^{-1}$ [21]. No characteristic peak corresponding to Al-O-Si linkage was observed in the FTIR spectra of the dried gel, which means both the aluminum hydroxide, $Al(OH)_3$ and silicon hydroxide, $Si(OH)_4$ formed under alkaline conditions precipitated simultaneously. So the precursor gel was diphasic in nature. The peak associated with Si-OH stretching was observed at 2855 $cm^{-1}$ in the spectra of the gel heated at 200 °C. In the spectra of the sample heated at 600 °C, the peak at 803 $cm^{-1}$ was assigned to symmetric stretching vibration of Si-O-Si linkages, which shifted slightly to 806 $cm^{-1}$ after heating at 800 °C. So Al-Si spinel started to form in the gel structure. The peak at 806 $cm^{-1}$ shifted to 832 $cm^{-1}$ in the spectra of the sample annealed at 1000 °C, indicating the formation of more Si-O-Al linkages resulting in the crystallization of mullite phases. At 1400 °C, peak at 843 $cm^{-1}$ became wider i.e. more Si-O-Al linkages started to form in the mullite crystals. After heating at 1600 °C, the peak corresponding to Si-O-Si linkage became broader, indicating complete crystallization of mullite [22, 23].

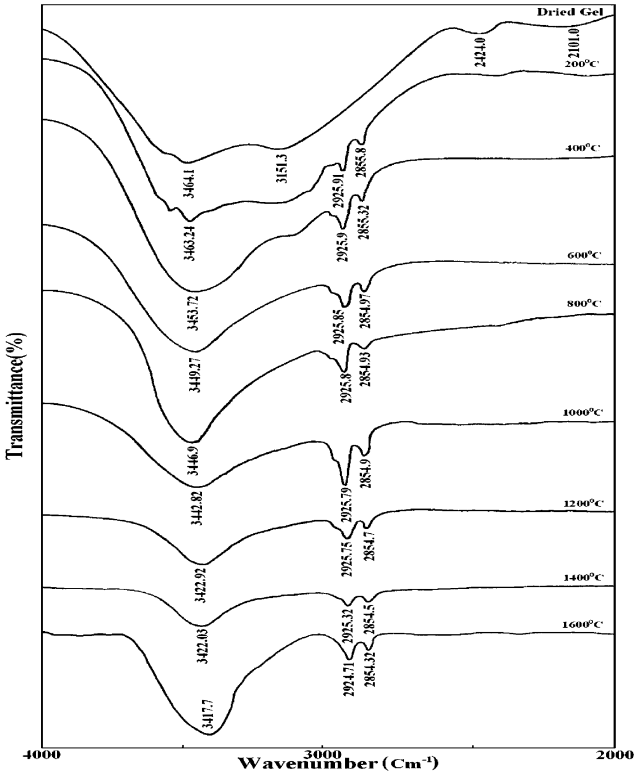


**Fig 1a:** FTIR spectra of the $Al_2O_3$-$SiO_2$ gel after heat treating at different temperatures within 2000 – 4000 $cm^{-1}$.

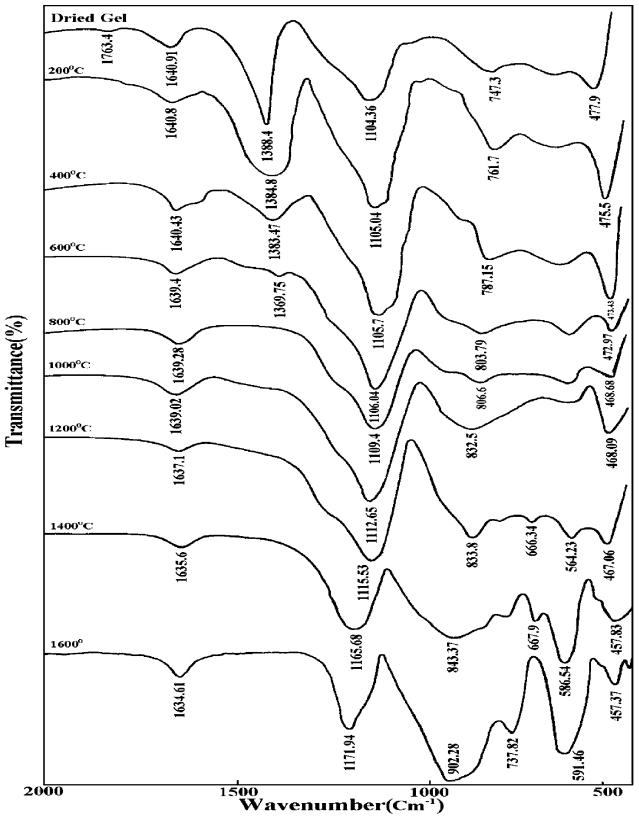


**Fig. 1b:** FTIR spectra of the $Al_2O_3$-$SiO_2$ gel after heat treating at different temperatures within 400 – 2000 $cm^{-1}$.

Differential thermal analysis of the gel was performed at multiple heating rates and from the curves it was observed that mullitization process was exothermic in nature (Fig. 2). With increasing heating rates, the peak temperatures shifted towards a higher temperature. Mullitization of the gel started in the temperature range 975 – 990 °C. The Kissinger equation was used to determine the activation energy of mullitization [24].

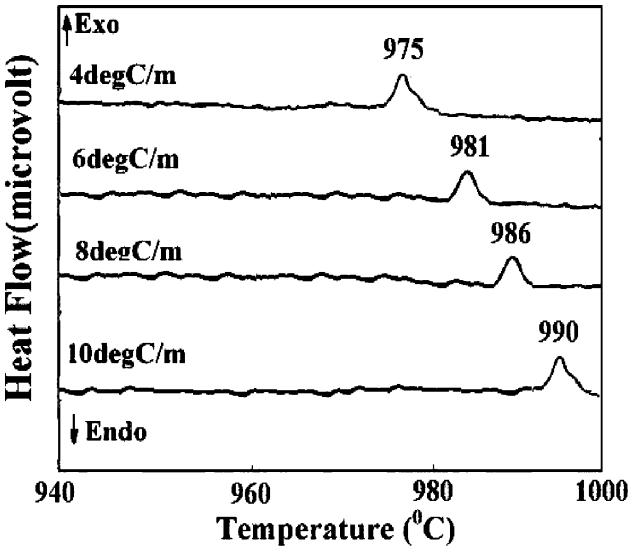


**Fig. 2:** DTA curves of the aluminosilicate gel at different heating rates.

The equation used is:

$$\ln\left(\frac{T_p^2}{\nu}\right) = \ln\left(\frac{E_a}{R}\right) - \ln\Phi + \frac{E_a}{RT_p} \qquad (1)$$

where, $T_p$ = temperature of the exothermic peak, $\nu$ = heating rate, $E_a$ = activation energy, R = universal gas constant and $\varphi$ = frequency factor (this is a constant dependent on the sample)

The plot of $\ln(T_p^2/\nu)$ versus $1/T_p$ will be a straight line and is shown in Fig. 3. The activation energy calculated from the slope of the line was equal to ~ 772 kJ/mol.

The x-ray diffractograms of the gel fired at 1400, 1500, and 1600 °C are shown in Fig. 4. Mullite was observed to be the major peaks followed by corundum. A certain amount of cristobalite was also observed in the microstructure. With the increase in the sintering temperature, the relative proportion of mullite phase increases in the microstructure.

The peak values obtained were compared with the standard JCPDS data (5 – 0776) and lattice parameters were calculated. The results obtained (Table 1) were compared with the values of unit cell parameters of orthorhombic mullite, a =7.60 Å, b =7.70 Å, c =2.90 Å [25 – 28]. At the sintering temperature of 1600 °C, the difference between the theoretical and experimentally obtained values of cell parameters was much lower compared with differences for the other two sintering temperatures. This can be related to the reduction in viscosity of the glassy phases around the mullite crystals. So with increased temperature, the structure became more perfect.

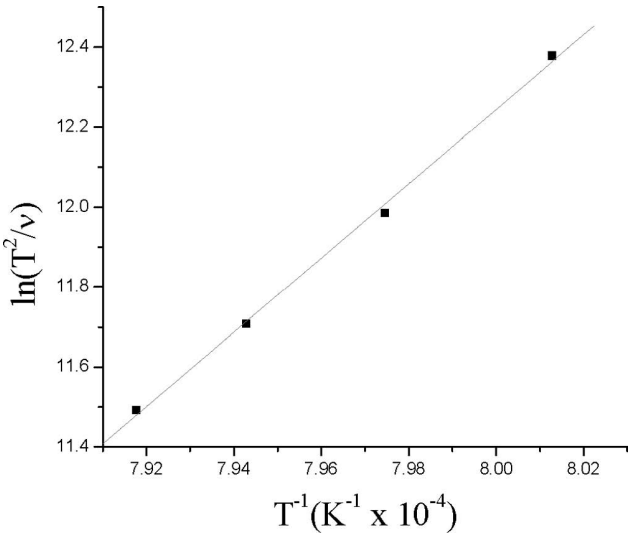


**Fig. 3:** Plot of ln ($T_p^2/\nu$) vs. $T^{-1}$ x $10^{-4}$ of the aluminosilicate gel.

After calculation of the lattice parameters, the volume of the crystallites were determined and it has also been observed that the difference in the crystallite volumes of the formed mullite from the theoretical values decreased as the sintering temperature was increased from 1400 to 1600 °C.

From the XRD data, the % d-error, which is a measure of the shift in mullite crystal planes owing to structural deformation and/or incomplete formation, was also calculated using the following formula:

$$\text{Relative percentage error, i.e. \%d error} = \frac{|d_{ex} - d|}{d} \times 100 \qquad (2)$$

where $d_{ex}$ is the actually obtained d value and d is the standard d-value in the JCPDS file.

**Table 1:** Values of lattice parameters of the gel sample at different sintering temperatures.

| Firing temperature (°C) | Theoretical cell parameters | | | | Experimental cell parameters | | | | Change in cell volume (%) |
|---|---|---|---|---|---|---|---|---|---|
| | a (Å) | b (Å) | c (Å) | abc (Å)$^3$ | a (Å) | b (Å) | c (Å) | abc (Å)$^3$ | |
| 1400 | 7.6 | 7.7 | 2.9 | 169.71 | 7.63 | 7.74 | 2.92 | 172.44 | 1.61 |
| 1500 | | | | | 7.61 | 7.72 | 2.91 | 170.96 | 0.74 |
| 1600 | | | | | 7.605 | 7.7 | 2.91 | 170.40 | 0.41 |

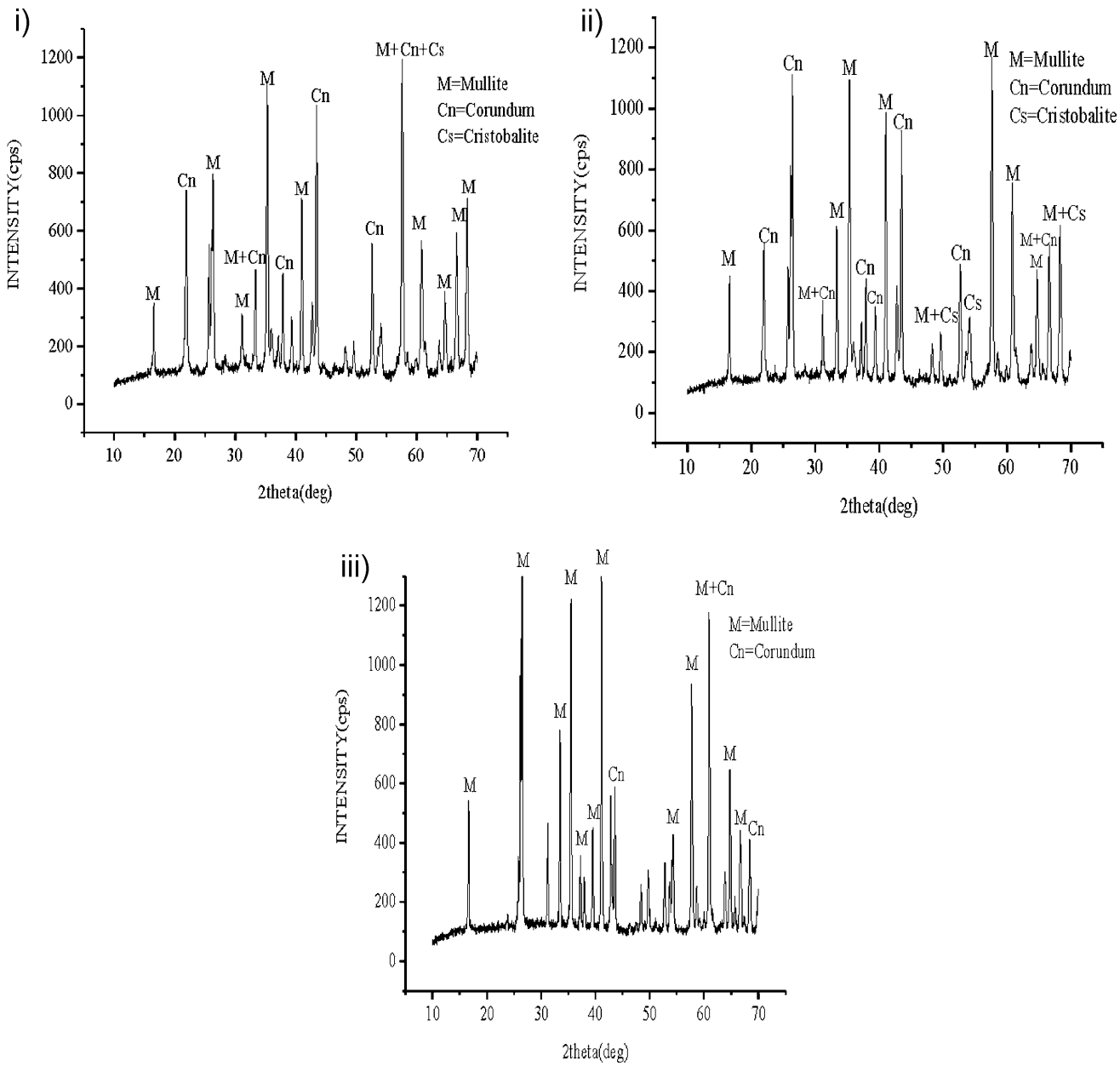


**Fig. 4:** XRD of the gel sample sintered at (i) 1400 °C (ii) 1500 °C (iii) 1600 °C.

The sums of the % d-error for mullite phase at the sintering temperature of 1400, 1500 and 1600 °C were observed to be 1.82 %, 1.78 % and 0.32 % respectively. From these values it is quite clear that with the increase in the sintering temperature from 1400 to 1600 °C the growth of mullite crystals became more and more effective and the crystal structure of the mullite became more perfect.

The average crystallite size was also calculated using Debye-Scherrer formula as follows:

$$D = 0.9\lambda/(\beta \cos\theta) \quad (3)$$

where D is the diameter of the crystallites forming the film, λ is the wavelength of CuKα line, β is full width at half-maximum (FWHM) in radians, and θ is the Bragg angle.

$$\beta = \sqrt{(\beta_0)^2 - (b)^2} \quad (4)$$

where $\beta_o$ is the FWHM in radians for the sample; b the FWHM in radians for the pure crystal.

The calculated crystallite sizes were observed to exist in the nano domain. The average particle sizes were found to be 22.38 nm, 26.18 nm and 29.28 nm at the sintering temperatures of 1400, 1500 and 1600 °C respectively. This indicates a positive influence of the sintering temperature on the growth of the crystallites.

## IV. Conclusions

Mullite ceramics were synthesized based on the colloidal interaction of silicic acid and $Al(NO_3)_3$ solution. The gel powder exhibited very low density and high surface area and consisted of separate non-linked units of alumina and silica gel. Primary mullitization started at around 980 °C with activation energy of ~772 kJ/mol. With increasing sintering temperature, mullitization became more effective and crystallization was completed after sintering at 1600 °C.

## References


1 Sola, E.R.D., Torres, F.J., Alarc, J.: Thermal evolution and structural study of 2: 1 mullite from monophasic gels, *J. Eur. Ceram. Soc.*, **26**, 2279 – 84, (2006).

2 Aksay, I.A., Pask, J.A.: Stable and metastable equilibria in system $SiO_2$-$Al_2O_3$, *J. Eur. Ceram. Soc.*, **58**, 507 – 12, (1975).

3 Klug, F.J., Prochazka, S., Doremus, R.H.: Alumina-silica phase diagram in the mullite region, *J. Am. Ceram. Soc.*, **70**, 750 – 59, (1987).

4 Ruscher, C.: Infra-red spectroscopic investigation in the mullite field of composition: $Al_2[Al_{2+2x}Si_{2-2x}]O_{10-x}$ with $0.55>x>0.25$, *J. Eur. Ceram. Soc.*, **16**, 169 – 75, (1996).

5 Schneider, H., Eberhard, E.: Thermal expansion of mullite, *J. Am. Ceram. Soc.*, **73**, 2073 – 76, (1990).

6 Hynes, A.P., Doremus, R.H.: High-temperature compressive creep of polycrystalline mullite, *J. Am. Ceram. Soc.*, **74**, 2469 – 75, (1991).

7 Kollenberg, W., Schneider, H.: Microhardness of mullite at temperartures to 1000 °C, *J. Am. Ceram. Soc.*, **72**, 1739 – 40, (1989).

8 Aksay, A., Dabbs, D.M., Sarikaya, M.: Mullite for structural, electronic and optical applications, *J. Am. Ceram. Soc.*, **74**, 2343 – 58, (1991).

9 Skoog, A.J., Moore, R.E.: Refractory of the past for the future: mullite and its use as a bonding phase, *Am. Ceram. Soc. Bull.*, **67**, 1180 – 85, (1988).

10 Ramakrishnan, V., Goo, E., Roldan, J.M., Giess, E.A.: Microstructure of mullite ceramics used for substrate and packaging applications, *J. Mater. Sci.*, **27**, 6127 – 30, (1992).

11 Mazel, F., Gonon, M., Fantozzi, G.: Manufacture of mullite substrates from andalusite for the development of thin film solar cells, *J. Eur. Ceram. Soc.*, **22**, 453 – 61, (2002).

12 Shinohara, N., Dabs, D.M., Aksay, I.A.: Infrared transparent mullite through densification of monolithic gels at 1250 °C, *Proc. SPIE—Int. Soc. Opt. Eng.*, **683**, 19 – 24, (1986).

13 Schneider, H.: Transition metal distribution in mullite, *Ceram. Trans.*, **6**, 135 – 138, (1990).

14 Cividanes, L.S., Campos, T.M.B., Rodrigues, L.A., Brunelli, D.D., Thim, G.P.: Review of mullite synthesis routes by sol-gel method, *J. Sol-Gel Sci. Technol.*, **55**, 111 – 25, (2010).

15 Padmaja, P., Anilkumar, G.M., Warrier, K.G.K.: Formation of mullite phase in diphasic gels consisting of TEOS and boehmite with and without dehydration, *J. Eur. Ceram. Soc.*, **18**, 1765 – 69, (1998).

16 Padmaja, P., Anilkumar, G.M., Warrier, K.G.K.: Characterization of stoichiometric sol-gel mullite by fourier transform infrared spectroscopy, *Int. J. Inorg. Mater.*, **3**, 693 – 98, (2001).

17 Yu, J., Shi, J., Yuan, Q., Yang, Z., Chen, Y.: Effect of composition on the sintering and microstructure of diphasic mullite gels, *Ceram. Int.*, **26**, 255 – 63, (2000).

18 Campos, A.L., Silva, N.T., Melo, F.C.L., Oliveira, M.A.S., Thim, G.P.: Crystallization kinetics of orthorhombic mullite from diphasic gels, *J. Non-Cryst. Solids.*, **304**, 19 – 24, (2002).

19 Buljan, I., Kosanovic, C., Kralj, D.: Novel synthesis of nanosized mullite from aluminosilicate precursors, *J. Alloy. Comp.*, **509**, 8256 – 61, (2011).

20 Roy, J., Das, S., Maitra, S.: Sol-gel-processed mullite coating – A review, Int. *J. Appl. Ceram. Technol.*, 1 – 7, DOI:10.1111/ijac.12230, (2014).

21 Okada, K., Otsuka, N.: Characterization of the spinel phase from $SiO_2$-$Al_2O_3$ xerogels and the formation process of mullite, *J. Am. Ceram. Soc.*, **69**, 652 – 56, (1986).

22 Orefice, B.L., Vasconcelos, W.L.: Sol-gel transition and structural evolution on multicomponent gels derived from the alumina-silica system, *J. Sol-Gel. Sci. Tech.*, **9**, 239 – 49 (1977).

23 Roy, J., Bandyopadhyay, N., Das, S., Maitra, S.: Studies on the formation of mullite from diphasic $Al_2O_3$-$SiO_2$ gel by fourier transform infrared spectroscopy, *Iran. J. Chem. Chem. Eng.*, **30**, 65 – 71, (2011).

24 Okada, K.: Activation energy of mullitization from various starting materials, *J. Eur. Ceram. Soc.*, **28**, 377 – 82, (2008).

25 Pask, J.A.: Importance of starting materials on reactions and phase equilibria in the $Al_2O_3$-$SiO_2$ system, *J. Eur. Ceram. Soc.*, **16,** 101 – 08, (1996).

26 Li, D.X., Thomson, W.J.: Mullite formation from non-stoichiometric diphasic precursors, *J. Am. Ceram. Soc.*, **74**, 2382 – 87, (1991).

27 Ossaka, J.: Tetragonal mullite-like phase from co-precipitated gels, *Nature*, **191**, 1000 – 01, (1961).

28 Li, D.X., Thomson, W.J.: Tetragonal to orthorhombic transformation during mullite formation, *J. Mater. Res.*, **6**, 819 – 43, (1991).